Anthropogenic forcing reduces predictability of decadal internal climate variability

Verjans, V.[1], Donat, M.[1,2], Palma, L.[1], and Delgado-Torres, C.[1]

1: Barcelona Supercomputing Center, Barcelona, Spain
2: Institució Catalana de Recerca i Estudis Avançats (ICREA), Barcelona, Spain

European Seminar on Computing (ESCO) 2026
Advanced Computational Methods for Earth System Modeling and Analysis

Funded by the European Union

Introduction: predictability

- Prediction ≠ Predictability
- Changes in predictability are well-documented on seasonal to inter-annual timescales.
- Variations in decadal predictability are less understood due to hindcasts availability only since 1960 (initialised climate models).
- Sea-surface temperature (SST) reanalysis data go back to ~1850.

- We use machine-learning to address:
  - Has decadal predictability changed over time?
  - If so, for which reasons?
  - Is future decadal predictability likely to change?

now be a desert. For our purposes we may therefore define climate in terms of the ensemble of all states during a long but finite time span. Climatic prediction then becomes the process of determining how these statistics will change as the beginning and end of the time span advance, and climatic predictability is concerned with whether such climatic prediction is possible.

Lorenz (1975)

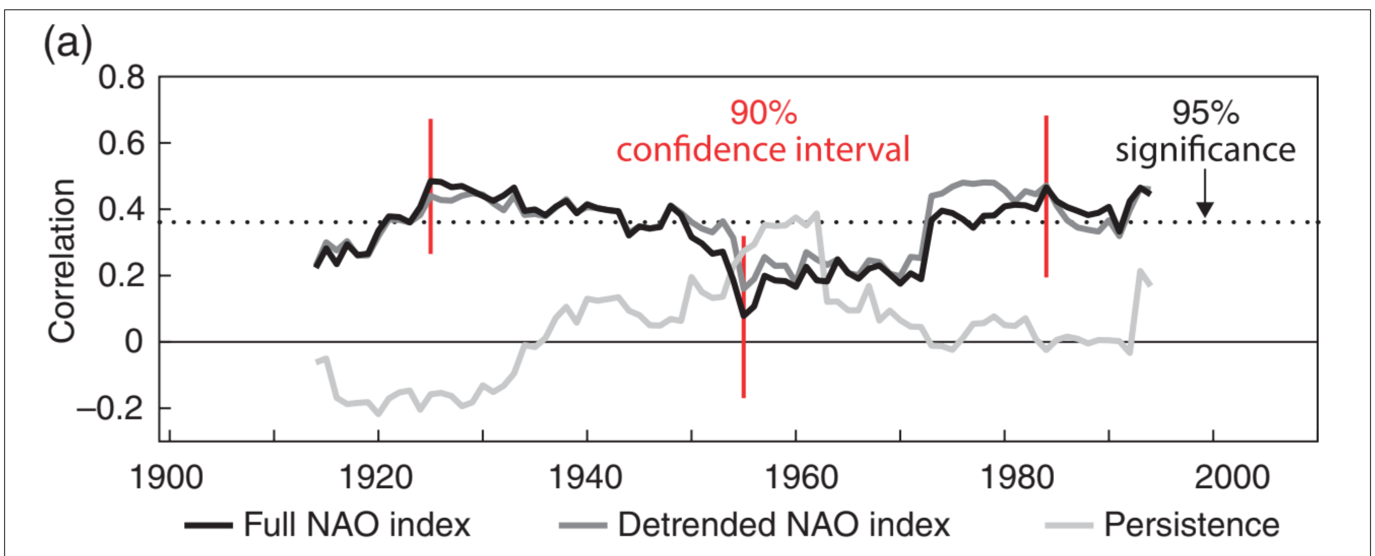

Illustration of variations in winter NAO seasonal predictability.

Weisheimer et al. (2017)

Methods: Learning residual decadal variability

- SST internal variability ("residuals"):
  $$x_t = \langle x_t \rangle + z_t \;\Rightarrow\; z_t = x_t - \langle x_t \rangle$$
  $$\langle x_t \rangle \approx \tilde{x}_t$$
- 12 CMIP6 models with ≥ 15 members
  historical simulations (1850-2014)
  SSP5-8.5 simulations (2015-2100)
- Train ML to predict forecast years 2-9 (8-year mean).
- Inputs: pre-forecast start: z_{t-}
  Outputs: 2-9 year mean: $\hat{z}_{2:9}$
  uncertainty: $\hat{\sigma}_{2:9}$
- Total: 491 historical simulations
  201 SSP5-8.5 simulations
- Train – Validation – Test split:
  70% - 15% - 15%

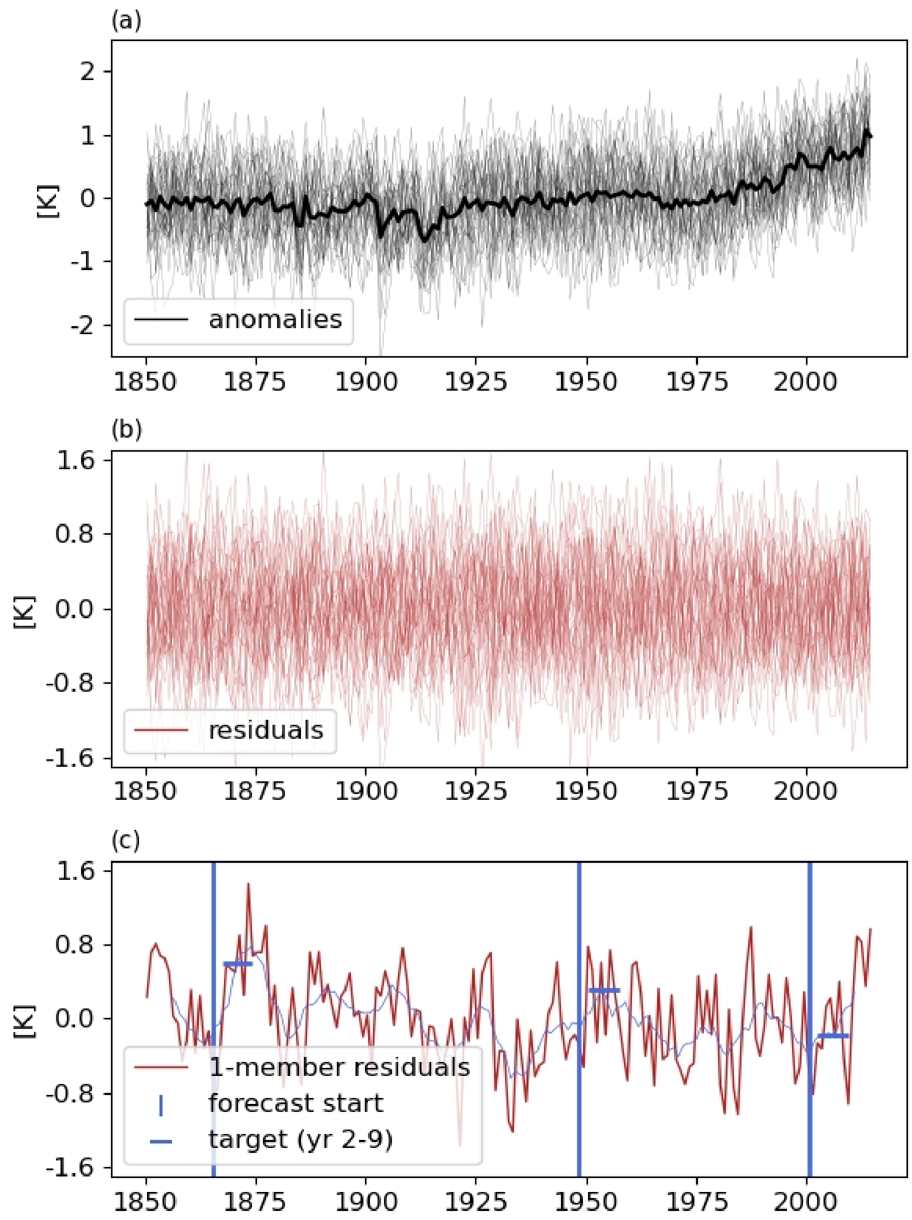

Example SST time series from the IPSL-CM6A-LR historical ensemble, at a grid cell in the central North Pacific.

Methods: Neural Network architecture

- ConvNeXt (Liu et al., 2022)
- Encoder-decoder convolutional neural network
  - Encoder: ↗ features, ↘ resolution
  - Decoder: ↗ resolution, maps to $\hat{z}_{2:9}, \hat{\sigma}_{2:9}$
- Both inputs and outputs are global maps

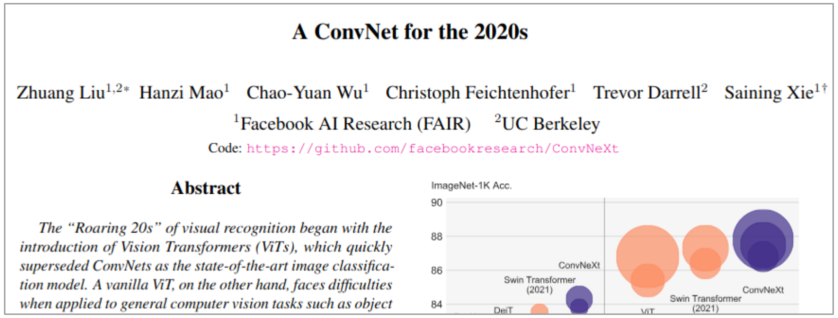

A ConvNet for the 2020s

Zhuang Liu[1,2*] Hanzi Mao[1] Chao-Yuan Wu[1] Christoph Feichtenhofer[1] Trevor Darrell[2] Saining Xie[1†]
[1]Facebook AI Research (FAIR) [2]UC Berkeley
Code: https://github.com/facebookresearch/ConvNeXt

Abstract

The "Roaring 20s" of visual recognition began with the introduction of Vision Transformers (ViTs), which quickly superseded ConvNets as the state-of-the-art image classification model. A vanilla ViT, on the other hand, faces difficulties when applied to general computer vision tasks such as object

- Probabilistic loss function:
  Continuous Rank Probability Score (CRPS)

- ConvNeXt blocks: residual blocks with 4× feature expansion, GELU, layer-wise convolutions

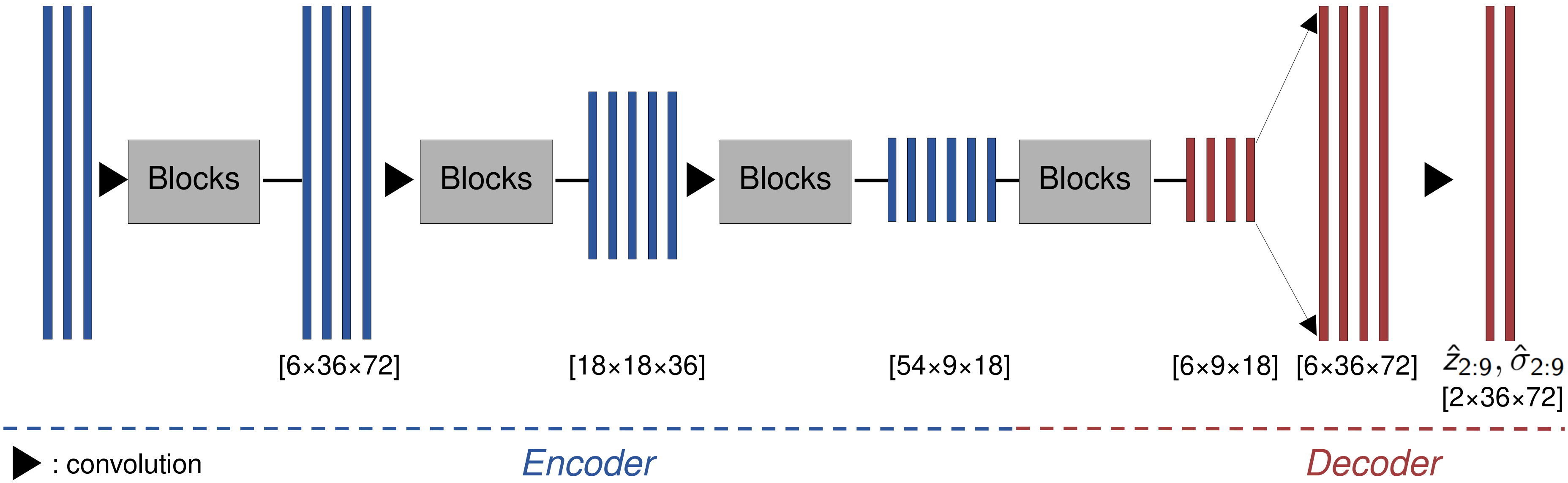

Evaluation: climate model predictions

- Evaluating correlation between true and predicted model residuals: $z_{2:9}$, $\hat{z}_{2:9}$
- North-Atlantic stands out in every model
- Other areas are model-dependent (North-Pacific, tropics …)
- Skill magnitude is model-dependent

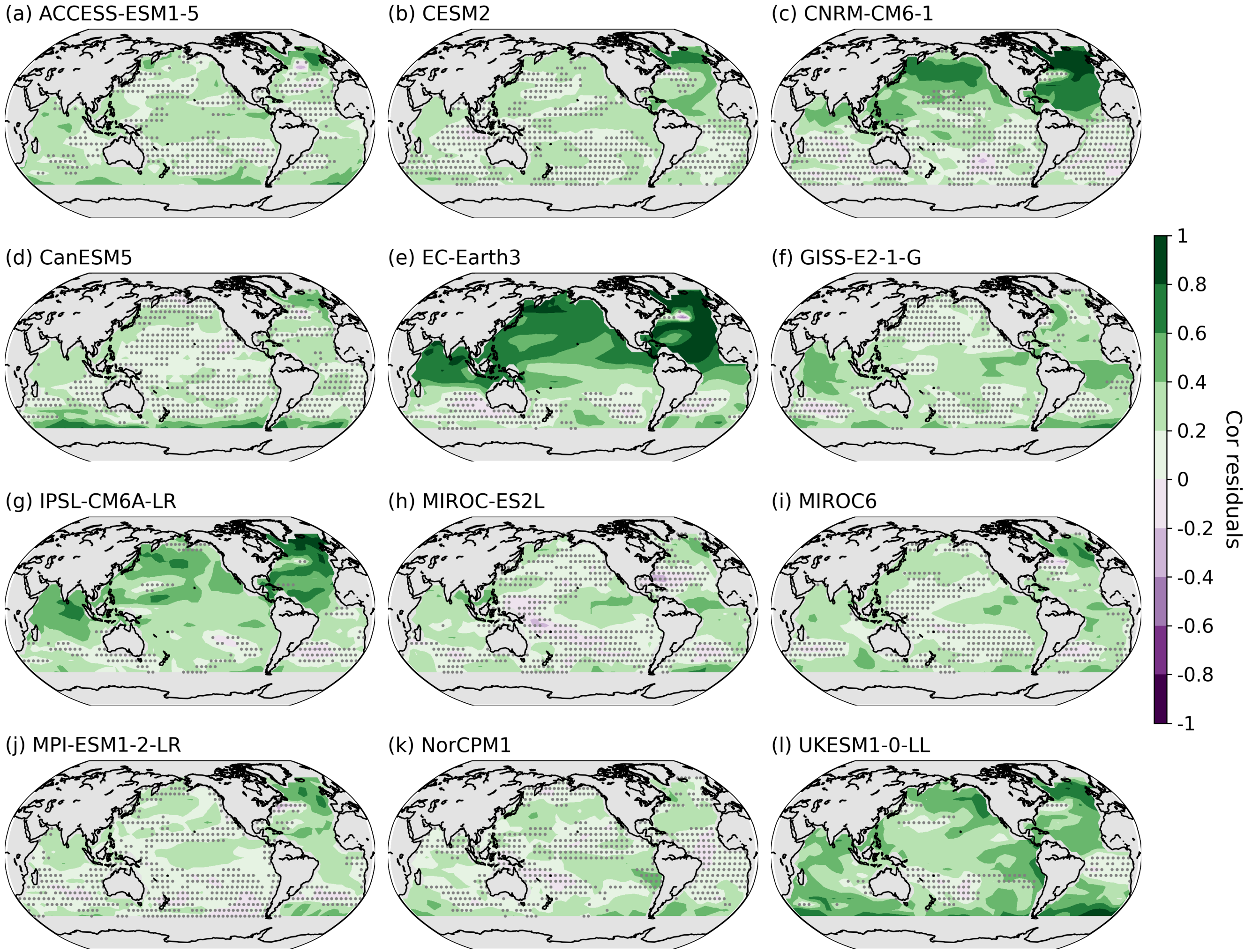

Notes: validation members only, shown is median ($\alpha = 0.10$)

Real-world hindcasts

- Application to real-world SST reanalysis data from ERSSTv6 (1850-2025)
- Comparison with an ensemble of initialised decadal predictions (DCPP, post-1960)

Evaluation: real-world hindcasts

- Positive correlations(North-Atlantic, North-Pacific …)
- Post-1960 ACC similar to DCPP
- ΔACC and CRPSS show skill comparable/exceeding that of DCPP

$$z_t = y_t - \tilde{y}_t$$
$$\text{ConvNeXt} \rightarrow \hat{z}_{2:9}, \hat{\sigma}_{2:9}$$
$$\hat{y}_{2:9} = \tilde{y}_{2:9} + \hat{z}_{2:9} \pm \hat{\sigma}_{2:9}$$

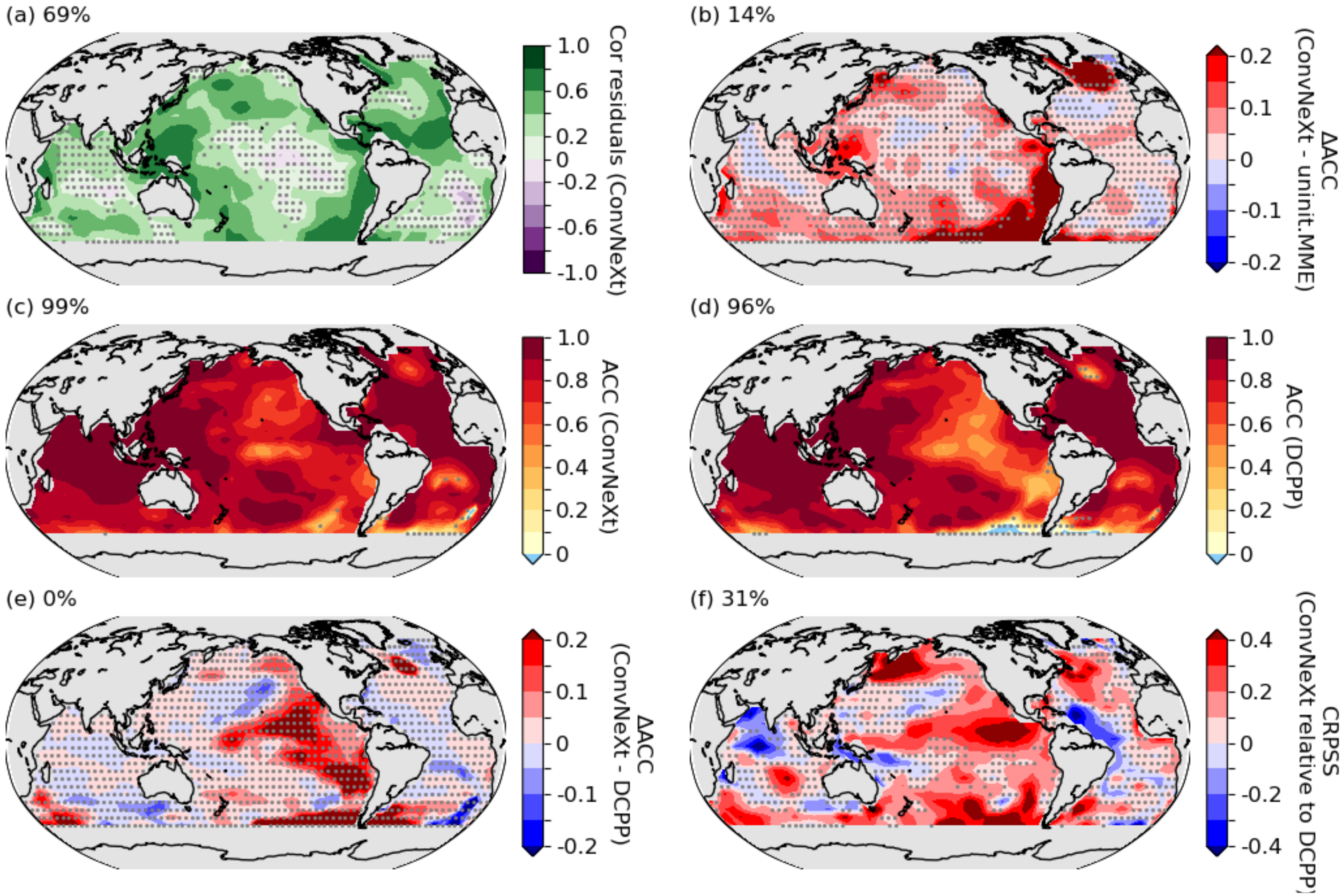


1850
P1
1950
P2
2025
P3
2100

Period separation

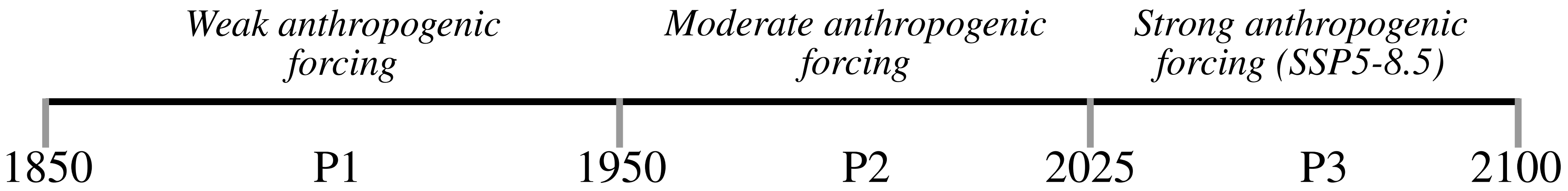

Changes in predictability

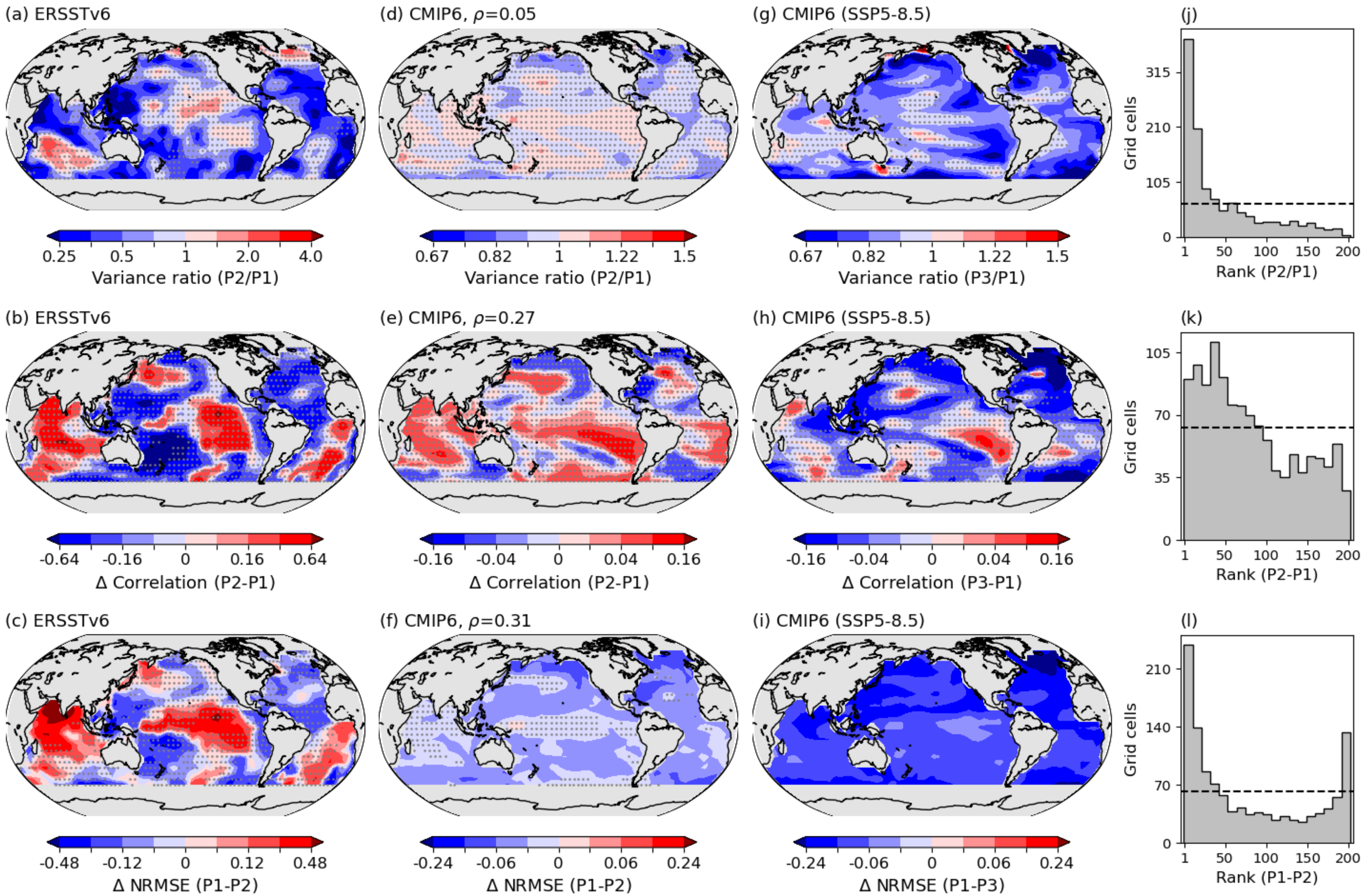

Changes in predictability

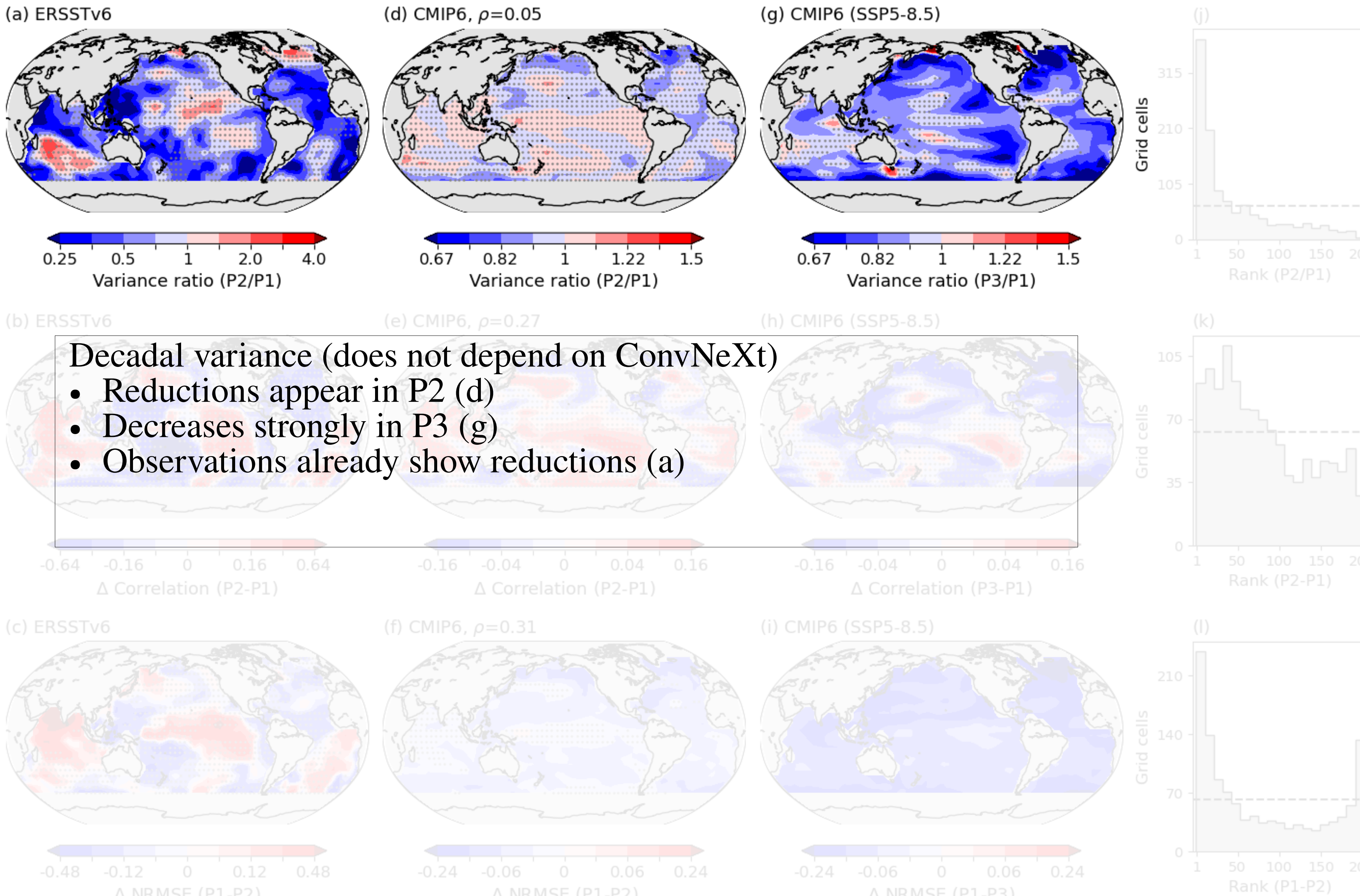

Decadal variance (does not depend on ConvNeXt)

- Reductions appear in P2 (d)
- Decreases strongly in P3 (g)
- Observations already show reductions (a)

Changes in predictability

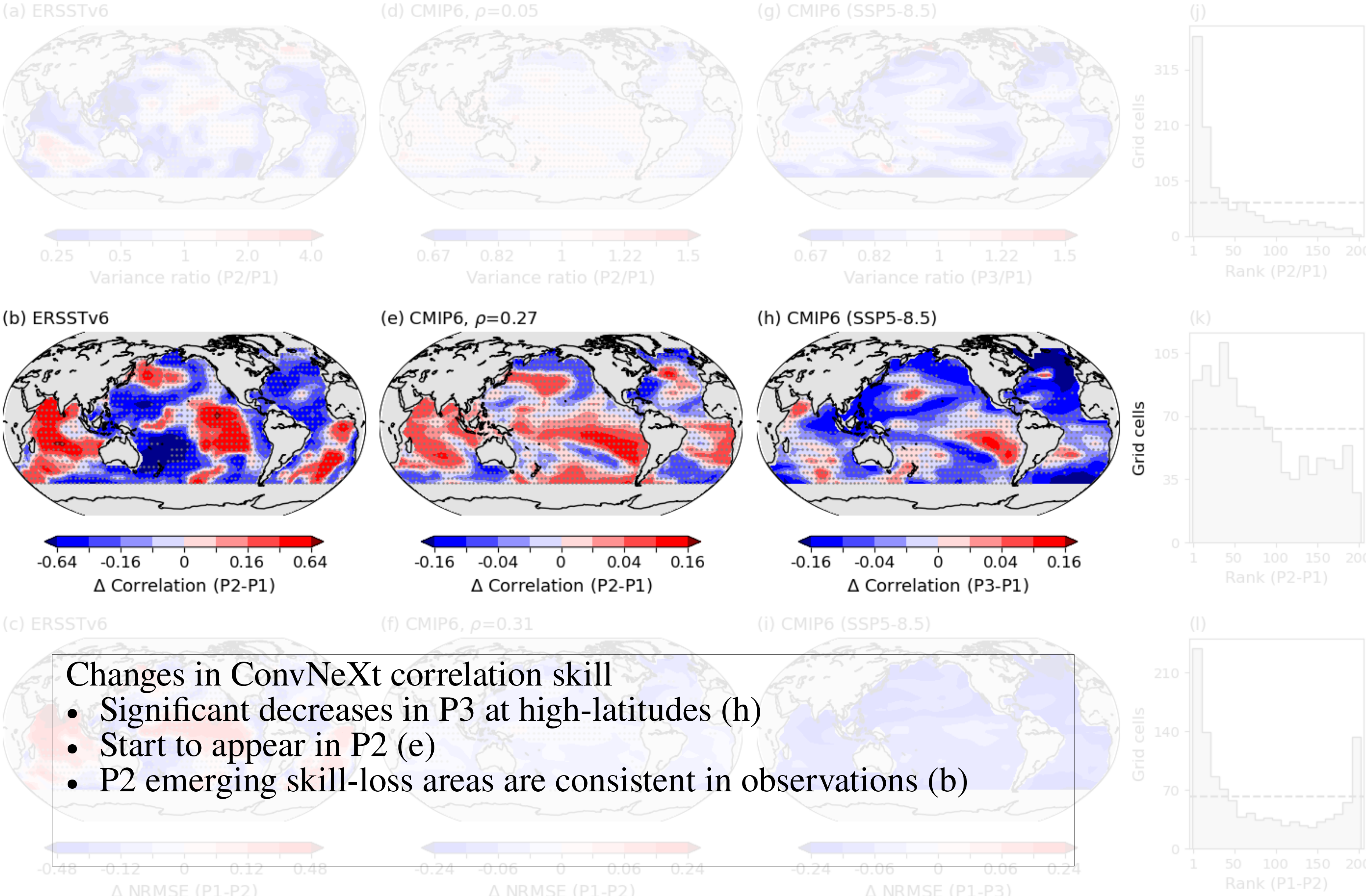

Changes in ConvNeXt correlation skill

- Significant decreases in P3 at high-latitudes (h)
- Start to appear in P2 (e)
- P2 emerging skill-loss areas are consistent in observations (b)

Changes in predictability

Changes in ConvNeXt NRMSE skill

- Combined effect of variance and error changes
- Widespread decrease in P3 (i) and P2 (f)
- Skill loss appears in observations in North-Atlantic and Pacific (c)

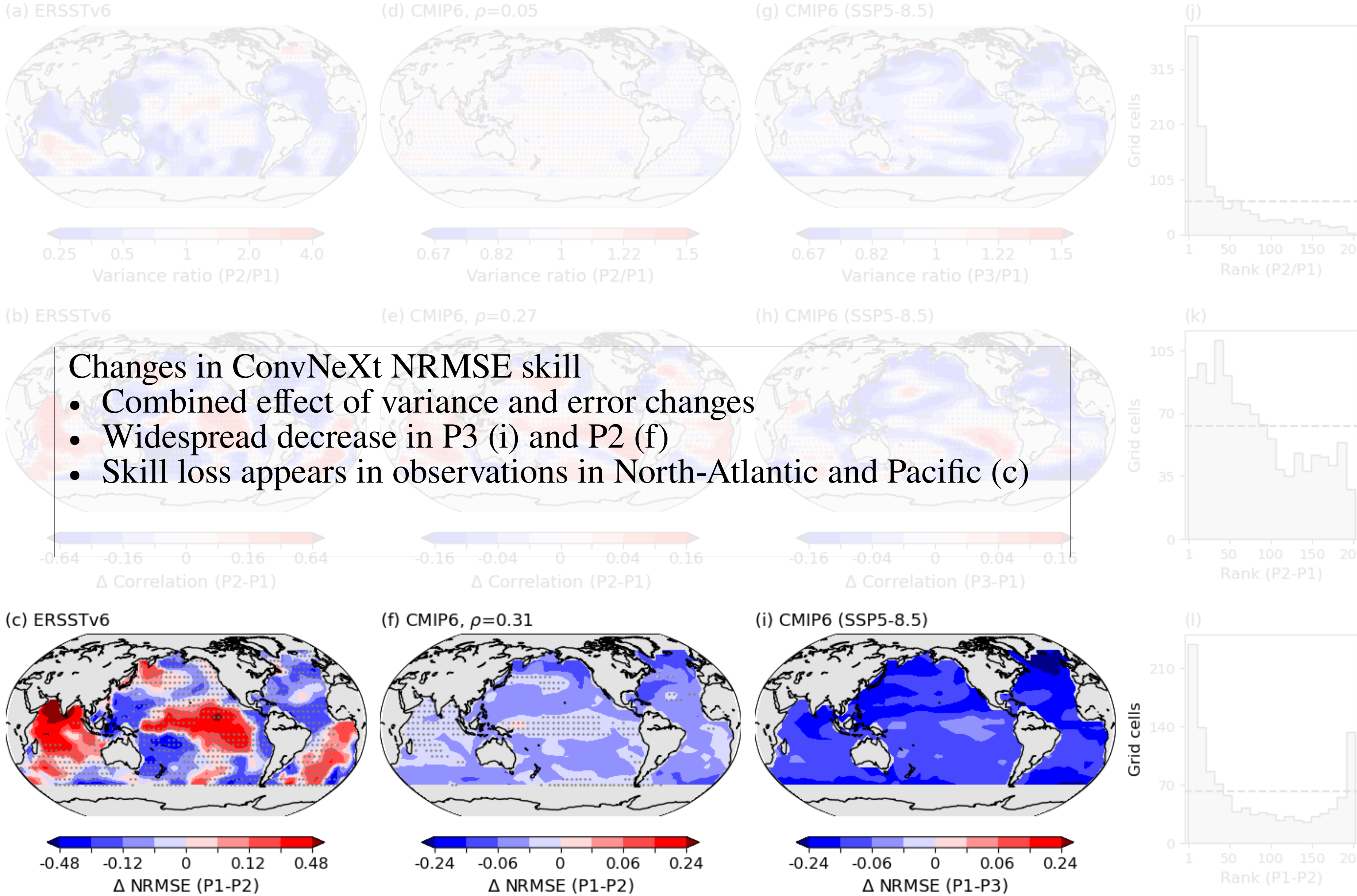

Changes in predictability

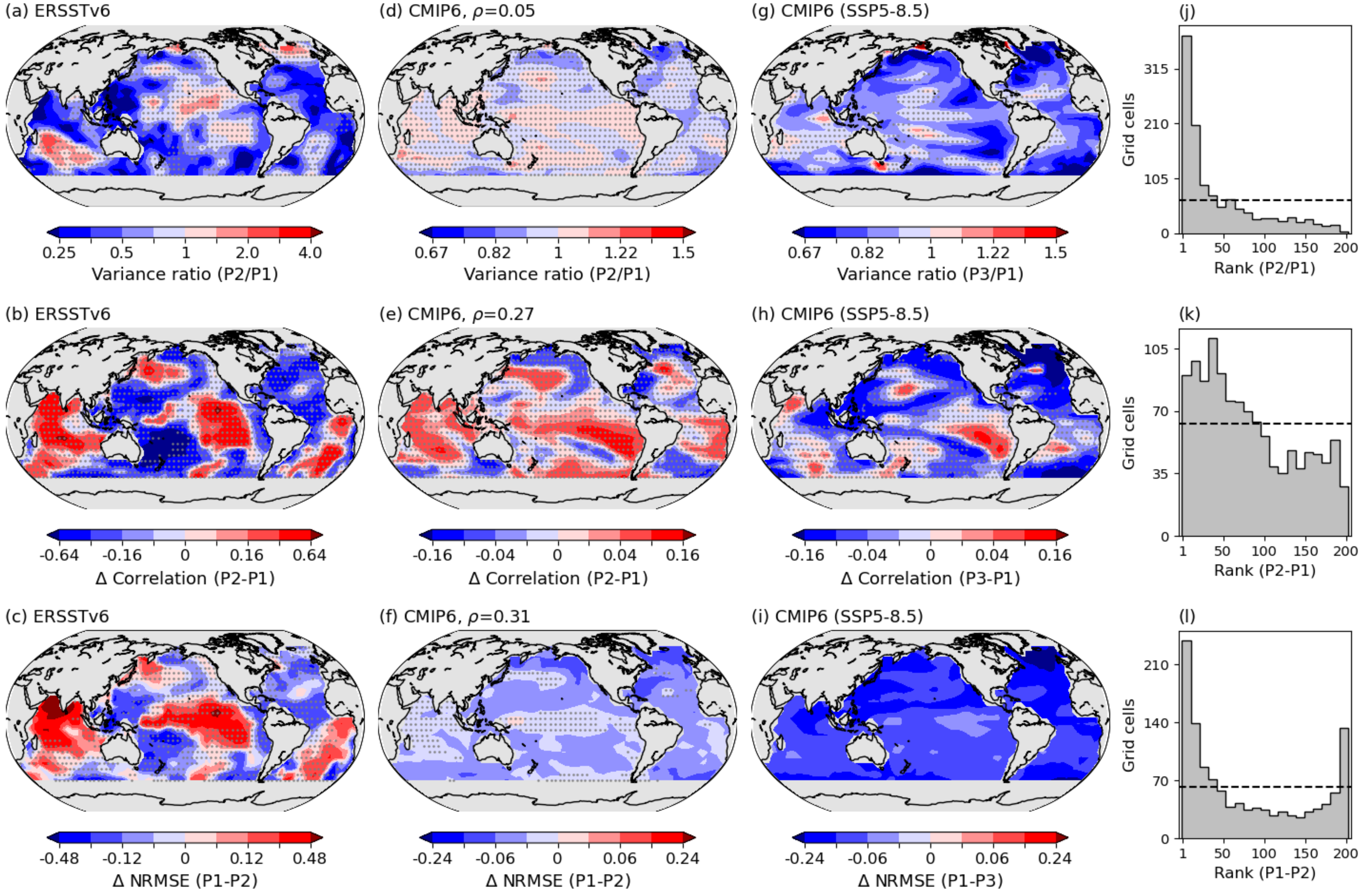

Conclusions

- A new ML-based decadal climate model requiring only SSTs, and predicting only SSTs.

- Skillful predictions of decadal SST internal variability, on par with skill of DCPP.

- Application to climate model simulations (1850-2100):
  - Strong reductions in decadal predictability for SSP5-8.5
  - Loss of predictability is generally accompanied by decadal variance decrease
  - These reductions start appearing in the later part of the historical period (1950-2025)

- Application to reanalysis (1850-2025):
  - Emergence of predictability reduction in decadal internal variability (pre- vs. post-1950)
  - Consistent with evolution seen in climate models, but with signs of a more rapid decrease

- Implications for decadal predictions in a warmer world

<u>Questions and comments are welcome</u>

BSC Barcelona Supercomputing Center
Centro Nacional de Supercomputación

vincent.verjans@bsc.es

EXPECT

Funded by the European Union

EXTRA SLIDES

Hindcasts
ERSSTv6

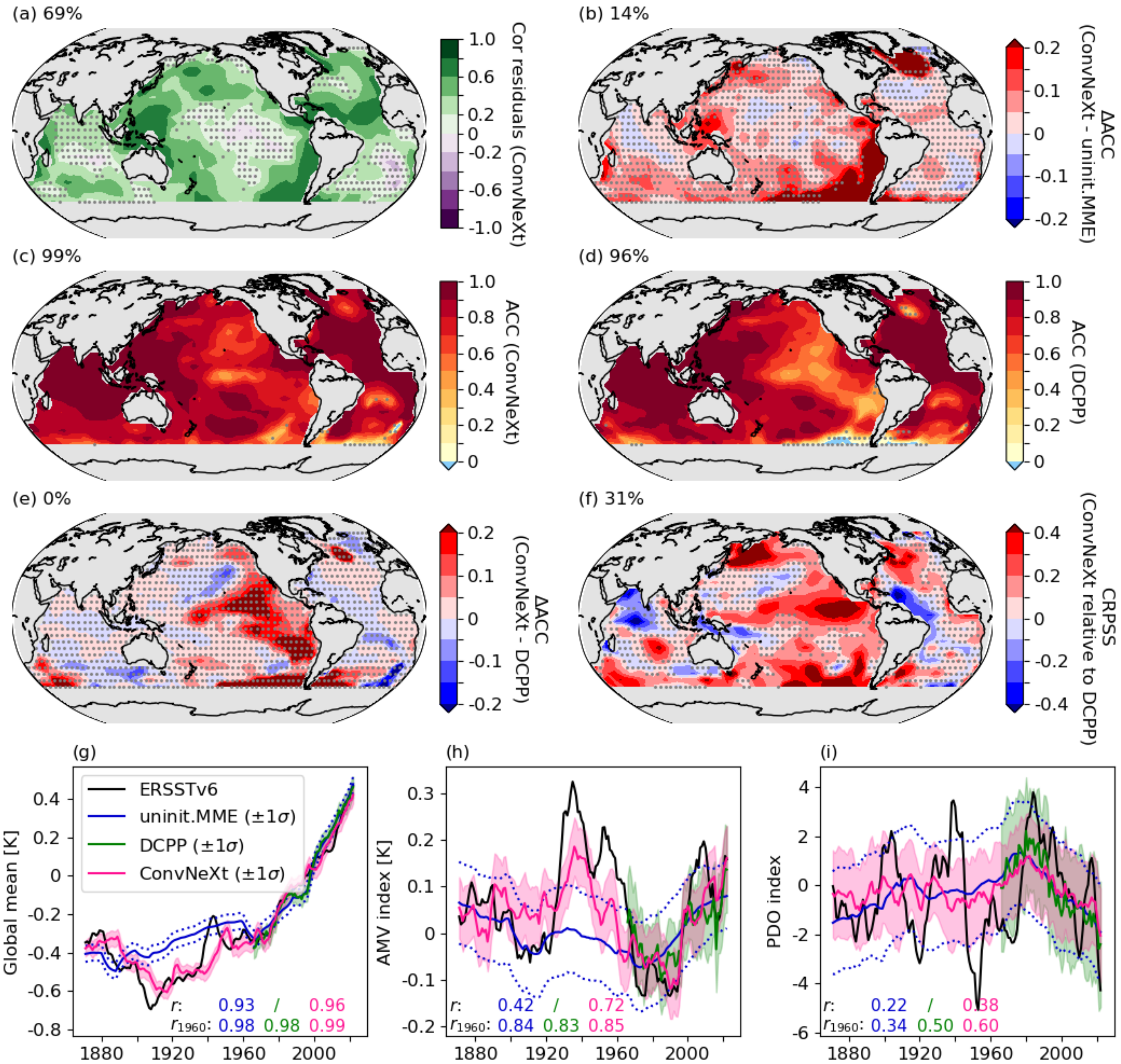

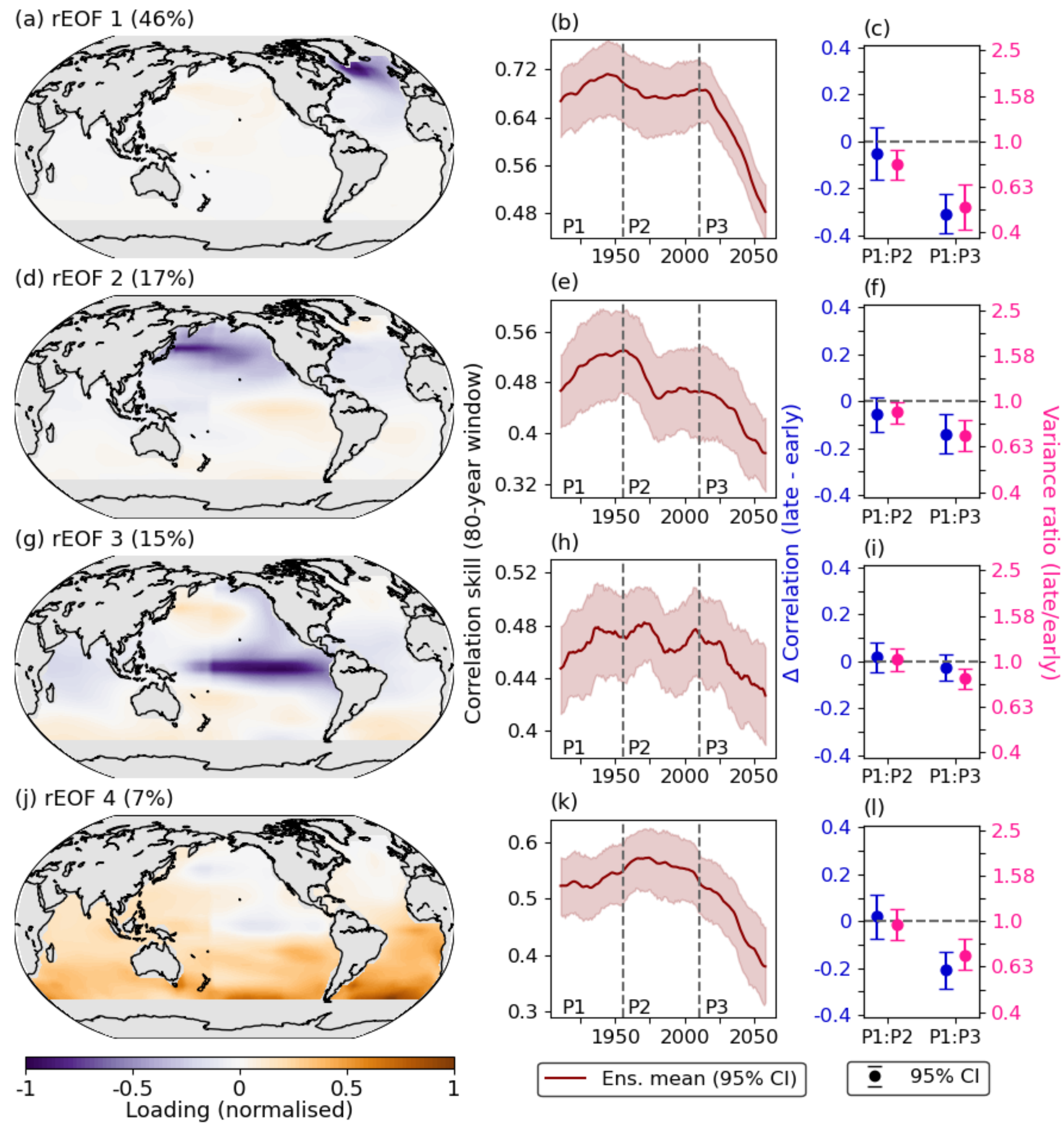

(a) rEOF 1 (46%)
(b)
(c)
(d) rEOF 2 (17%)
(e)
(f)
(g) rEOF 3 (15%)
(h)
(i)
(j) rEOF 4 (7%)
(k)
(l)
P1
P2
P3
1950
2000
2050
P1:P2
P1:P3
Correlation skill (80-year window)
Δ Correlation (late - early)
Variance ratio (late/early)
Loading (normalised)
Ens. mean (95% CI)
95% CI

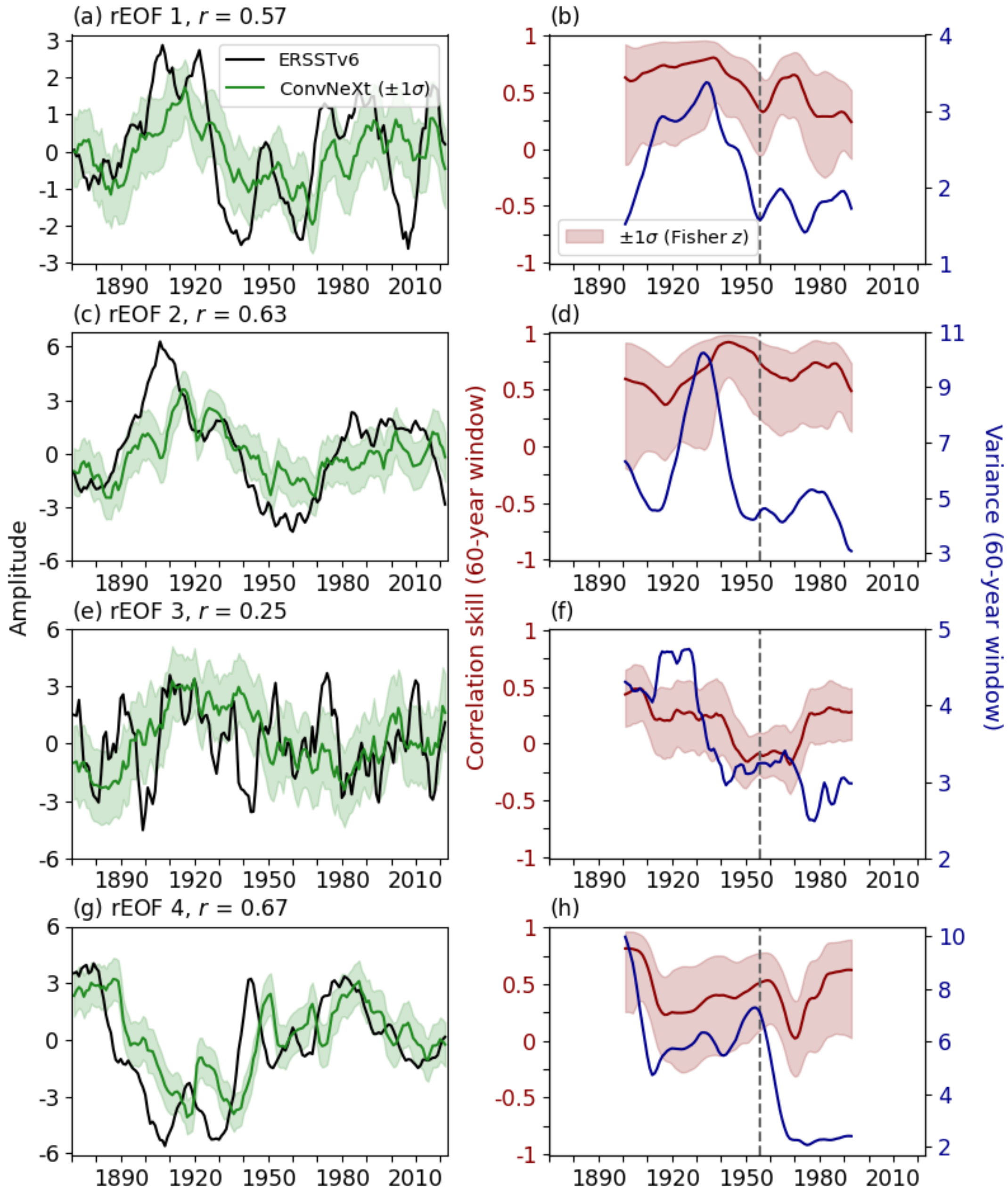
(a) rEOF 1, r = 0.57
(b)
(c) rEOF 2, r = 0.63
(d)
(e) rEOF 3, r = 0.25
(f)
(g) rEOF 4, r = 0.67
(h)
ERSSTv6
ConvNeXt (±1σ)
±1σ (Fisher z)
Amplitude
Correlation skill (60-year window)
Variance (60-year window)
1890
1920
1950
1980
2010

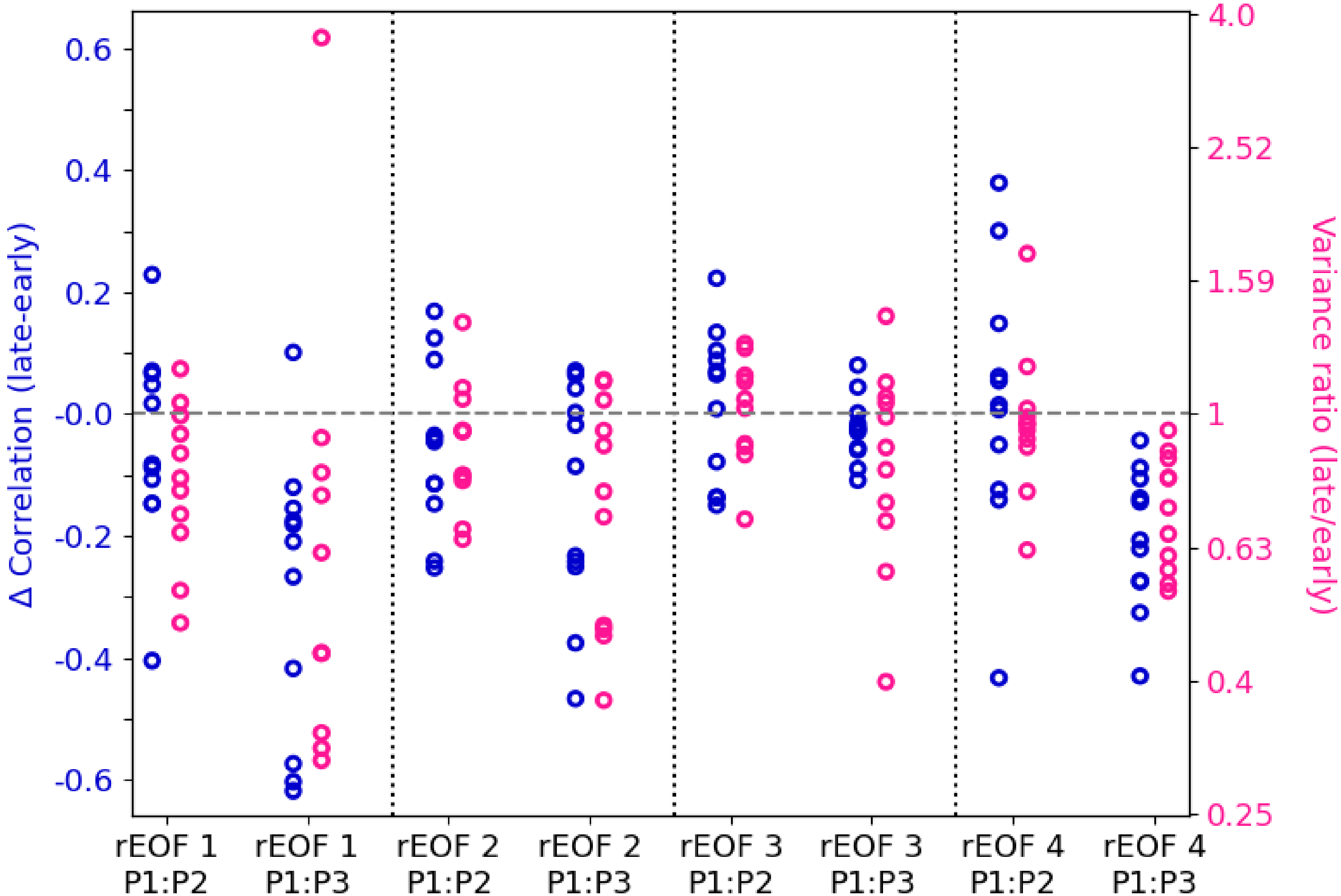

0.6
0.4
0.2
-0.0
-0.2
-0.4
-0.6
Δ Correlation (late-early)
4.0
2.52
1.59
1
0.63
0.4
0.25
Variance ratio (late/early)
rEOF 1 P1:P2
rEOF 1 P1:P3
rEOF 2 P1:P2
rEOF 2 P1:P3
rEOF 3 P1:P2
rEOF 3 P1:P3
rEOF 4 P1:P2
rEOF 4 P1:P3

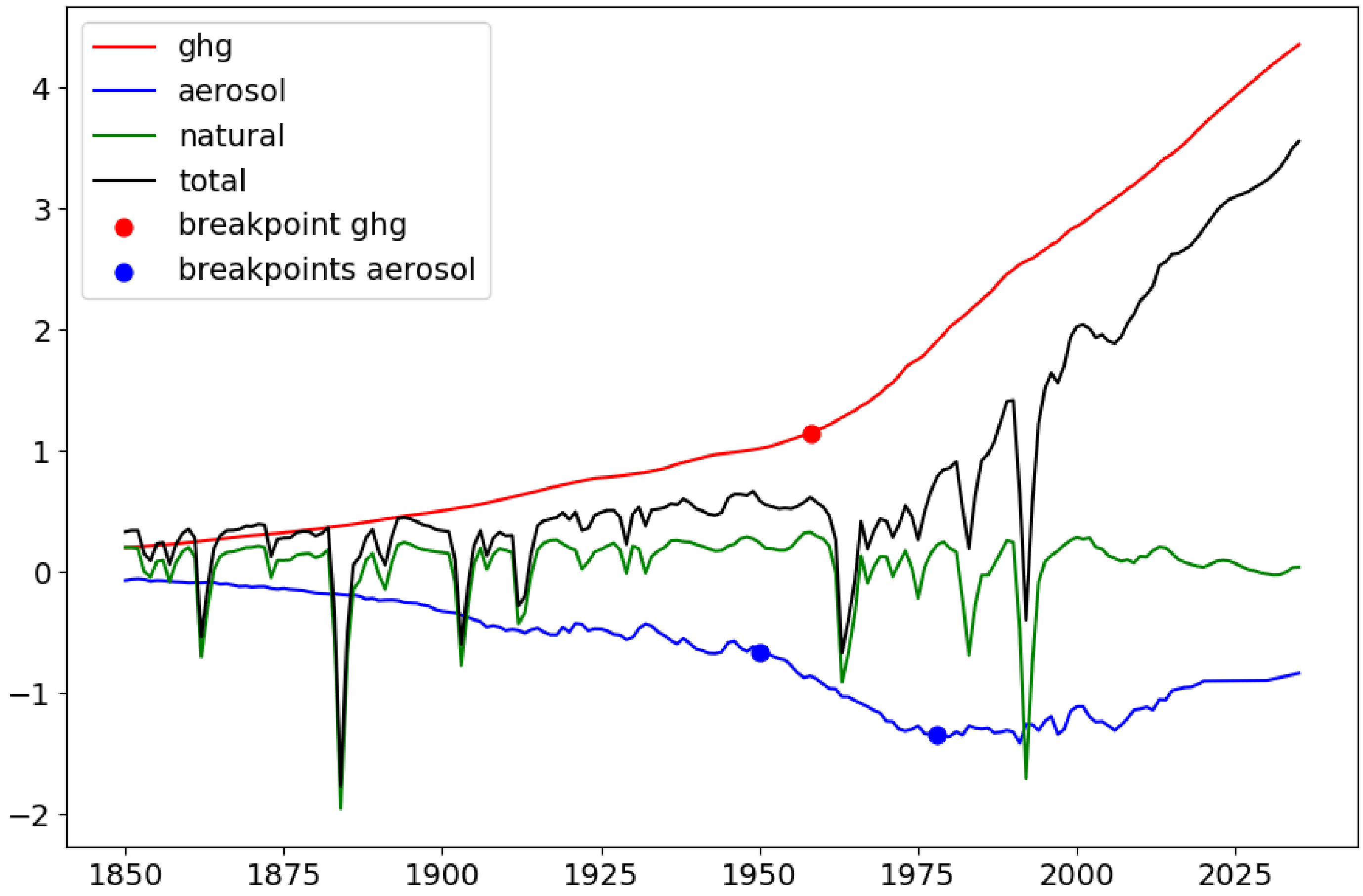

ghg
aerosol
natural
total
breakpoint ghg
breakpoints aerosol
4
3
2
1
0
−1
−2
1850
1875
1900
1925
1950
1975
2000
2025

Hindcasts
COBE2

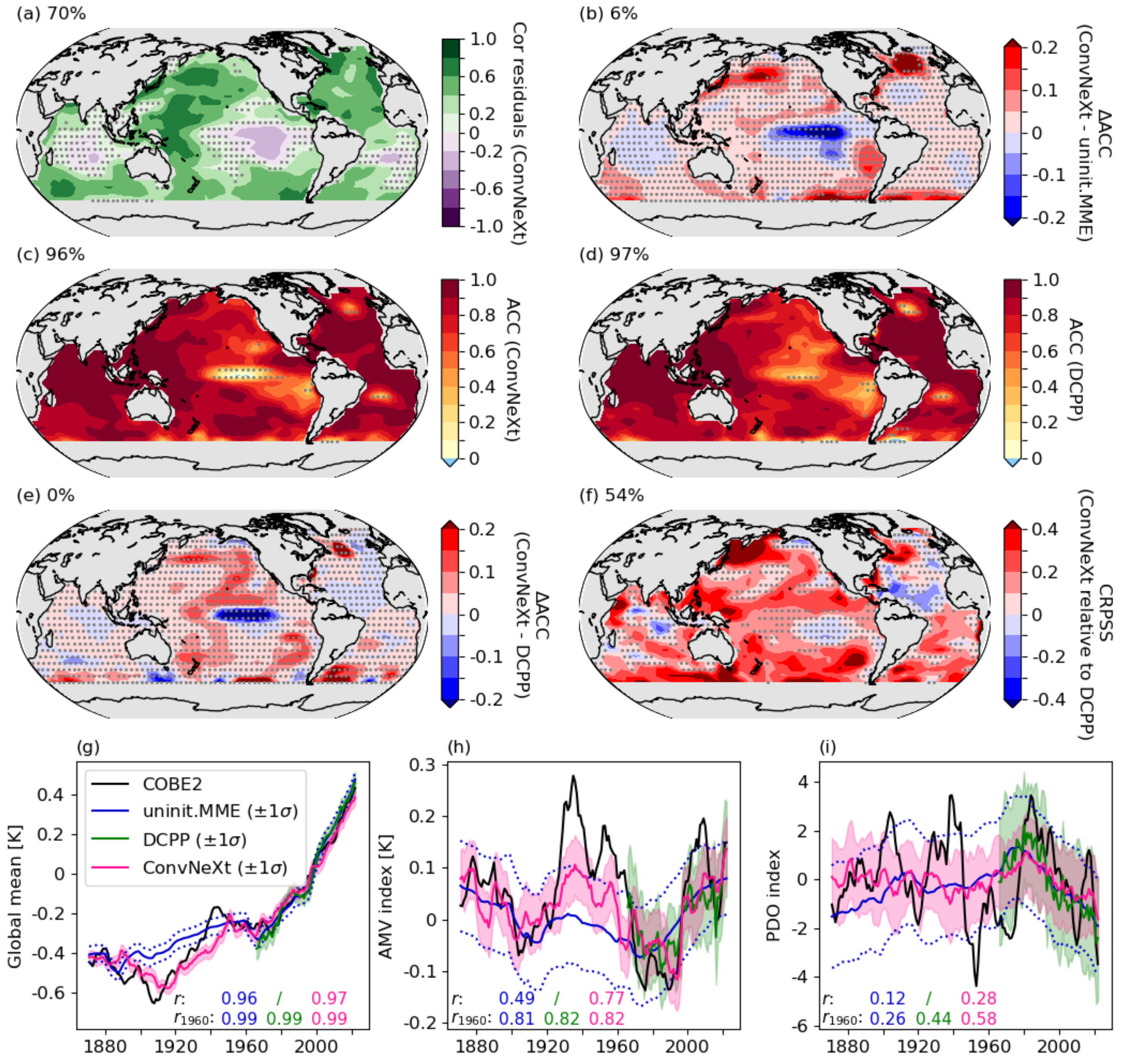

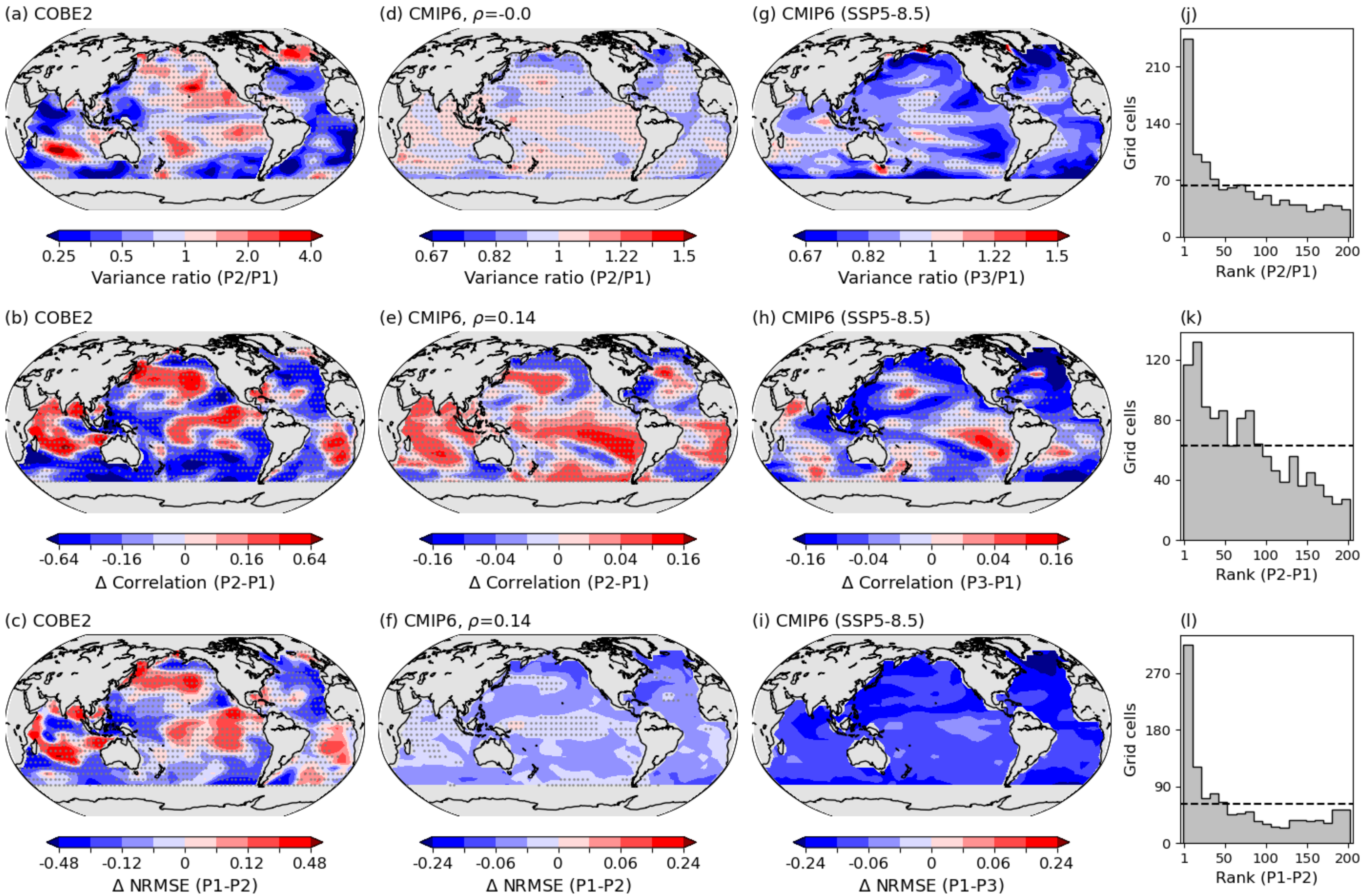

(a) COBE2
(d) CMIP6, ρ=-0.0
(g) CMIP6 (SSP5-8.5)
(j)
0.25 0.5 1 2.0 4.0
Variance ratio (P2/P1)
0.67 0.82 1 1.22 1.5
Variance ratio (P2/P1)
0.67 0.82 1 1.22 1.5
Variance ratio (P3/P1)
Grid cells
Rank (P2/P1)
(b) COBE2
(e) CMIP6, ρ=0.14
(h) CMIP6 (SSP5-8.5)
(k)
-0.64 -0.16 0 0.16 0.64
Δ Correlation (P2-P1)
-0.16 -0.04 0 0.04 0.16
Δ Correlation (P2-P1)
-0.16 -0.04 0 0.04 0.16
Δ Correlation (P3-P1)
Rank (P2-P1)
(c) COBE2
(f) CMIP6, ρ=0.14
(i) CMIP6 (SSP5-8.5)
(l)
-0.48 -0.12 0 0.12 0.48
Δ NRMSE (P1-P2)
-0.24 -0.06 0 0.06 0.24
Δ NRMSE (P1-P2)
-0.24 -0.06 0 0.06 0.24
Δ NRMSE (P1-P3)
Rank (P1-P2)

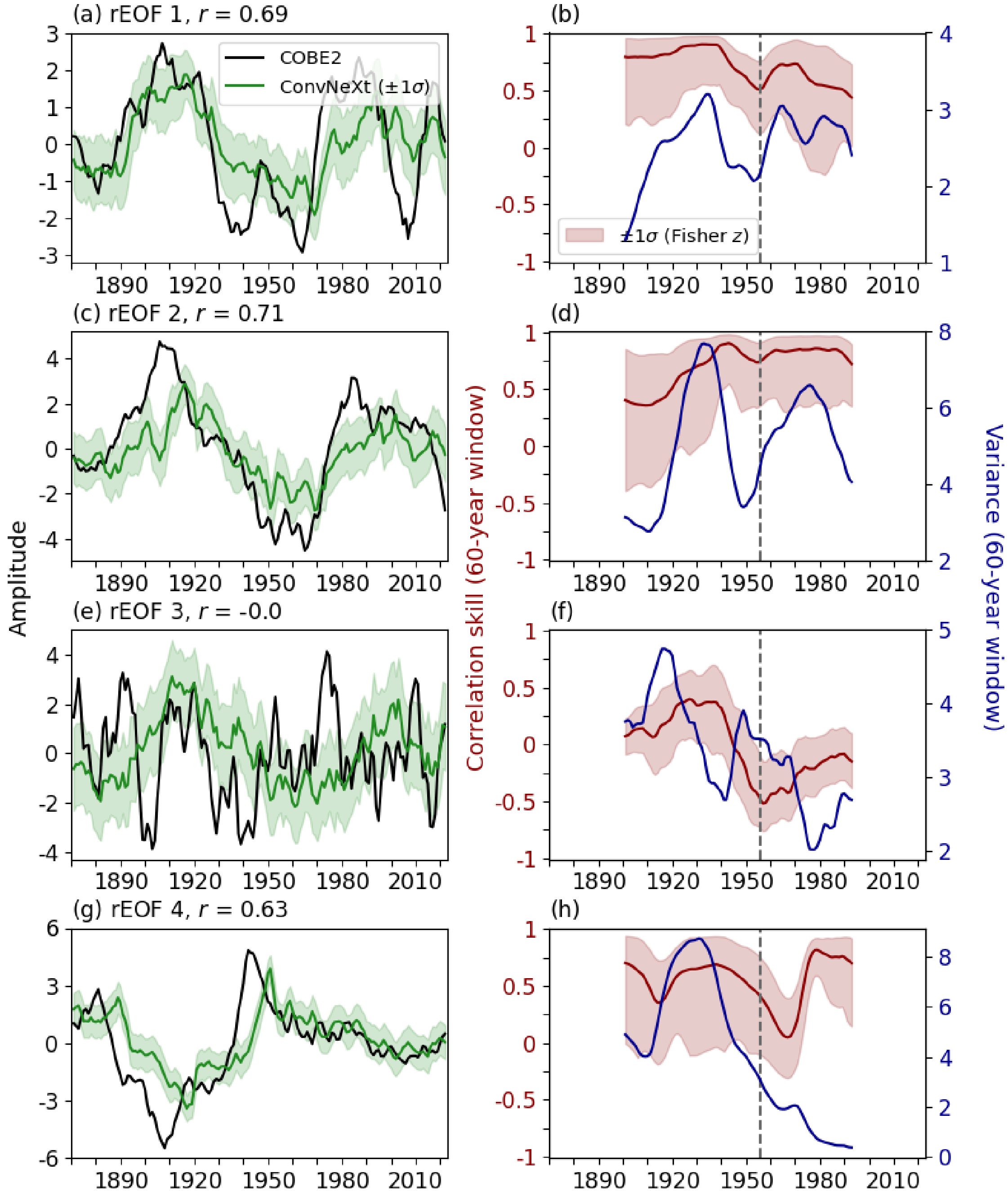

(a) rEOF 1, r = 0.69
COBE2
ConvNeXt (±1σ)
(b)
±1σ (Fisher z)
(c) rEOF 2, r = 0.71
(d)
(e) rEOF 3, r = -0.0
(f)
(g) rEOF 4, r = 0.63
(h)
Amplitude
Correlation skill (60-year window)
Variance (60-year window)
1890
1920
1950
1980
2010

Model	$\mathrm{N_{hist}}$	$\mathrm{N_{ssp585}}$
ACCESS-ESM1-5	40	40
CESM2	100	5
CNRM-CM6-1	30	6
CanESM5	65	50
EC-Earth3	22	5
GISS-E2-1-G	46	14
IPSL-CM6A-LR	32	6
MIROC-ES2L	30	10
MIROC6	50	50
MPI-ESM1-2-LR	30	10
NorCPM1	30	0
UKESM1-0-LL	16	5
Total	491	201

$$\mathrm{CRPS}(\mathbf{y}, \hat{\mathbf{y}}, \hat{\boldsymbol{\sigma}}) = \hat{\boldsymbol{\sigma}} \left[\frac{-1}{\sqrt{\pi}} + \frac{\mathbf{y} - \hat{\mathbf{y}}}{\hat{\boldsymbol{\sigma}}} \mathrm{erf}\left(\frac{\mathbf{y} - \hat{\mathbf{y}}}{\sqrt{2}\hat{\boldsymbol{\sigma}}} \right) + \sqrt{\frac{2}{\pi}} \exp\left(\frac{-(\mathbf{y} - \hat{\mathbf{y}})^2}{2\hat{\boldsymbol{\sigma}}^2} \right) \right]$$